

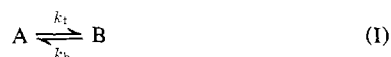
# Kinetically Controlled Association–Dissociation Reactions on Gel Chromatography†

James K. Zimmerman

**ABSTRACT:** Theoretical reaction boundaries for gel chromatography have been generated for several reversible macromolecular association–dissociations under kinetic control. These patterns show that if a system is initially at equilibrium, kinetic control will be expressed when the half-time of the first-order (dissociation) rate constant is near one order of magnitude of the time the macromolecules have been on the column. In at least one case, the change in the reaction profile

is greatest when the first-order half-time is equal to the residence time but the effect is still observable as long as the reaction half-time is within an order of magnitude of the time the experiment has been running. Flow rates have been varied to determine whether this method may be used to obtain kinetic constants from experimental curves. In addition, a computer program has been developed which can handle the interactions, in any form, of any four species.

In all types of transport systems the question of what is a slow reaction or an instantaneous reaction in relation to the time of duration of the experiment is critical in the analytical evaluation of the observed boundary profiles (Longworth and MacInnes, 1942). Many analytical expressions have been derived (Gilbert, 1955, 1959; Gilbert and Jenkins, 1956, 1959) and numerous computer simulations (Cox, 1965, 1967, 1969, 1971; Cann, 1970; Cann and Goad, 1965, 1972; Bethune and Kegeles, 1961; Zimmerman and Ackers, 1971a, 1971b, 1973; Zimmerman *et al.*, 1971) have been done using the assumption of instantaneous equilibrium between species. It is, therefore, necessary to establish whether or not “instantaneous equilibrium” can be assumed under reasonable conditions and rates. Early work on kinetically controlled reactions by Van Holde (1962) and others on isomerizing systems of the type



and Belford and Belford (1962) for dimerizations



was undertaken without including effects of dispersion (diffusion). Oberhauser *et al.* (1965) extended the dimerization case by including dispersion for countercurrent distribution. Recently a paper by Cann and Oates (1973) has delineated some of these limits for the sedimentation velocity and electrophoresis patterns of certain irreversible macromolecular reactions. Halvorson and Ackers (1973) have evaluated methods for determining kinetic constants for isomerization using small zone elution chromatography. However, in none but the Halvorson and Ackers system do the dispersion effects play as large a role as in gel chromatography (Zimmerman *et al.*, 1971; Zimmerman and Ackers, 1971a).

This paper shows the effect of reversible reactions on systems initially in an equilibrium state and perturbed from equilibrium by passage through a gel chromatography column. By main-

taining a constant ratio of rate constants corresponding to the equilibrium state one may determine at what values of these rate constants the resulting profiles approach the limiting cases of (1) instantaneous equilibrium and (2) no interaction.

Three different cases of a monomer–tetramer reaction and one case of a monomer–dimer reaction were chosen as representative systems. These systems may be described by reaction 3, where  $P_1$  represents a monomer,  $P_n$  the  $n$ -mer,  $k_t$



the association rate constant, and  $k_b$  the dissociation rate constant. At equilibrium, this system may be described by

$$K_{eq} = P_n/P_1^n = k_t/k_b \quad (1)$$

## Methods

All of the computer programs used in this paper were direct modifications of the programs previously described by Zimmerman and Ackers (1971a, 1971b, 1973) and Zimmerman *et al.* (1971) based on the method of Cox (1965, 1967, 1969, 1971).<sup>1</sup> Results were calculated on an IBM 370/155 digital computer. These programs allow the user to describe the reaction profiles resulting from the flow equation for gel chromatography (Zimmerman and Ackers, 1971a) as in eq 2,

$$J' = u_T C_T' - L_T \frac{dC_T'}{dX} \quad (2)$$

where  $J'$  is the flow of mass per unit time per unit area,  $u_T$  is the weight average velocity of all the components,  $C_T'$  is the total concentration with respect to the column frame of reference (Zimmerman and Ackers, 1971a; Brumbaugh and Ackers, 1968) which is the concentration detected by the gel

† From the Department of Biochemistry, Clemson University, Clemson, South Carolina 29631. Received August 20, 1973.

<sup>1</sup> Many of the independent modifications of the Cox program have resulted in some parts of the program looking somewhat like those employed by Cann and Goad (1965, 1972) as described in Cann (1970). The current approach still resembles the Cox program more than that of Cann and Goad.

TABLE I: System Parameters for Gel Chromatography Simulations.

Stoichiometry	Gel	$\sigma_1$	$\sigma_n$	$L_1$ (cm <sup>2</sup> /min)	$L_n$ (cm <sup>2</sup> /min)	Radius of $n$ -mer (ångströms)
1-4	G-200R	0.714	0.474	$3.61 \times 10^{-4}$	$4.86 \times 10^{-4}$	30.0
1-2	G-100R	0.570	0.324	$8.89 \times 10^{-4}$	$5.66 \times 10^{-4}$	23.8

scanning chromatograph of Ackers (Brumbaugh and Ackers, 1968),  $L_T$  is the gradient average dispersion coefficient, and  $X$  is the distance parameter.

The weight average velocity,  $u_T$ , and gradient average dispersion coefficient,  $L_T$ , may be written as

$$u_T = \frac{F \sum C_j' / \xi_j}{\sum C_j'} \quad (3)$$

and

$$L_T = \frac{\sum L_j \frac{dC_j'}{dX}}{\sum \frac{dC_j'}{dX}} \quad (4)$$

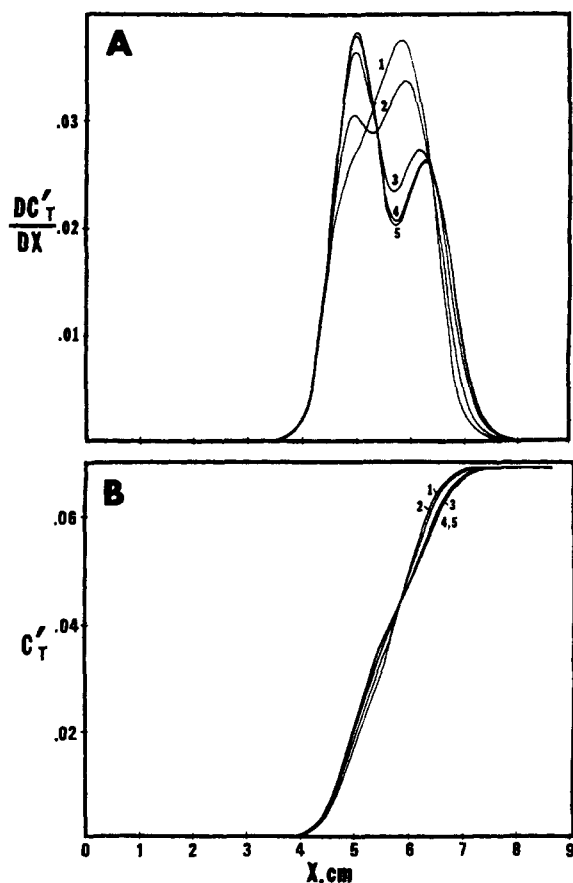


FIGURE 1: Computer simulation of a monomer-tetramer system on Sephadex G-200R. Reaction profiles after 192 min at a flow rate of 1.2 ml/hr with an initial loading concentration of 0.1 mg/ml (50% tetramer by weight). Interaction parameters are (1) instantaneous equilibrium  $K_{eq} = 8000$  (mg/ml)<sup>-3</sup>. The same curve is generated by  $k_f = 800$  (mg/ml)<sup>-3</sup> min<sup>-1</sup>,  $k_b = 0.1$  min<sup>-1</sup>; (2)  $k_f = 80$  (mg/ml)<sup>-3</sup> min<sup>-1</sup>,  $k_b = 0.01$  min<sup>-1</sup>; (3)  $k_f = 8$  (mg/ml)<sup>-3</sup> min<sup>-1</sup>,  $k_b = 0.001$  min<sup>-1</sup>; (4)  $k_f = 0.8$  (mg/ml)<sup>-3</sup> min<sup>-1</sup>,  $k_b = 10^{-4}$  min<sup>-1</sup>; (5) no interaction. Curves A are derivatives of concentration profiles B.

where the subscript  $j$  refers to the  $j$ th component,  $F$  is the flow rate, and  $\xi_j$  is a dimensionless parameter reflecting the fraction of the volume available to solute molecule  $j$  (Zimmerman and Ackers, 1971a). The parameter  $\xi$  in turn reflects the size of the solute molecule (Ackers, 1970) with the larger molecule having the smaller  $\xi$ . The phenomenological value of interest is the partition coefficient,  $\sigma$  (Ackers, 1970), related to  $\xi$  by

$$\xi = \alpha + \beta\sigma \quad (5)$$

where  $\alpha$  and  $\beta$  are dimensionless parameters related to the fraction of volume available to the void volume and internal volume respectively.

The physical model is that of a uniformly packed column of unit cross sectional area. At time zero the column is saturated with solute creating a step function at position  $X = 0$ . The column is divided into a series of boxes and it is the contents of each of these boxes that is monitored. At the appropriate

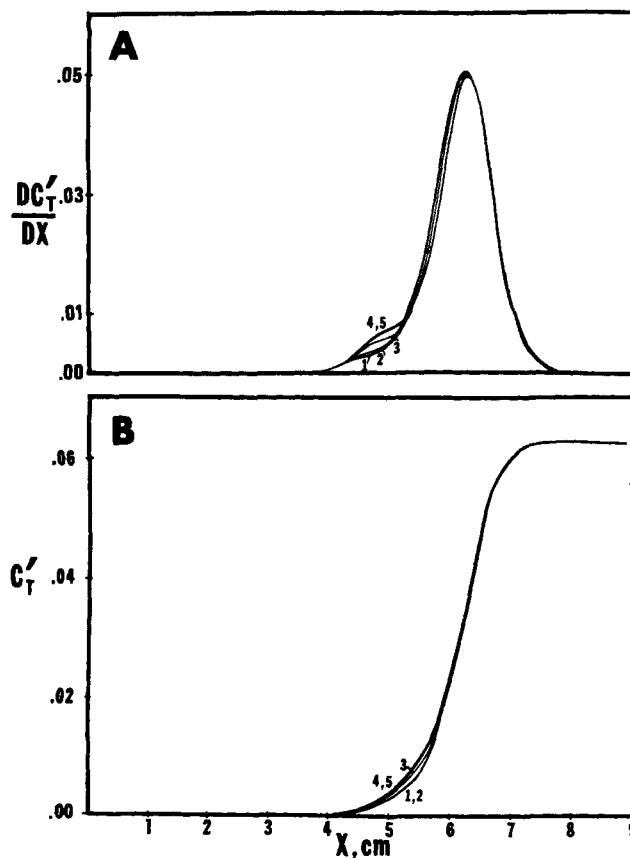


FIGURE 2: Effect of initial concentration of tetramer. Same conditions as in Figure 1 but with the initial mixture containing 90% tetramer. Interaction parameters are (1) instantaneous equilibrium,  $K_{eq} = 9 \times 10^6$  (mg/ml)<sup>-3</sup>; (2)  $k_f = 90,000$  (mg/ml)<sup>-3</sup> min<sup>-1</sup>,  $k_b = 0.01$  min<sup>-1</sup>; (3)  $k_f = 9000$  (mg/ml)<sup>-3</sup> min<sup>-1</sup>,  $k_b = 0.001$  min<sup>-1</sup>; (4)  $k_f = 900$  (mg/ml)<sup>-3</sup> min<sup>-1</sup>,  $k_b = 10^{-4}$  min<sup>-1</sup>; (5) no interaction. Curves A are derivatives of concentration profiles B.

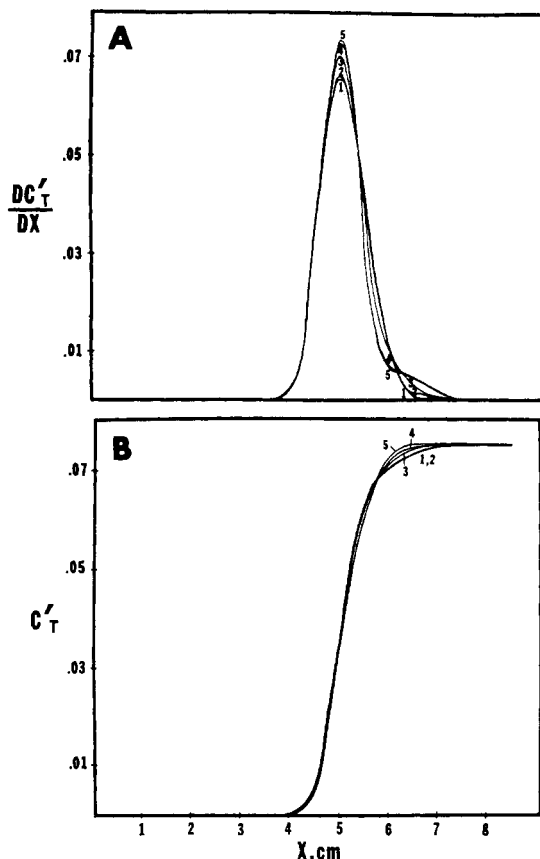


FIGURE 3: Effect of initial concentrations of tetramer. Same conditions as in Figure 1 but with 10% tetramer in the initial mixture. Interaction parameters are (1) instantaneous equilibrium,  $K_{eq} = 152 \text{ (mg/ml)}^{-3}$ ; (2)  $k_t = 15.2 \text{ (mg/ml)}^{-3} \text{ min}^{-1}$ ,  $k_b = 0.1 \text{ min}^{-1}$ ; (3)  $k_t = 1.52 \text{ (mg/ml)}^{-3} \text{ min}^{-1}$ ,  $k_b = 0.01 \text{ min}^{-1}$ ; (4)  $k_t = 0.152 \text{ (mg/ml)}^{-3} \text{ min}^{-1}$ ,  $k_b = 0.001 \text{ min}^{-1}$ ; (5) no interaction. Curves A are derivatives of concentration profiles B.

times the contents of each box is recorded and the reaction profile of the resulting trailing boundary is generated.

In previous papers the final reaction profile was determined by alternating rounds of translation and dispersion where each translation step was followed by several dispersion steps to minimize the change in distribution for any one dispersion step. In this paper, when kinetic control is simulated, there exists within each dispersion step several kinetic steps, set so that a minimum amount of reaction occurs during each step. In effect there are three loops in the program. Within each transport loop the dispersion loop cycles several times and within each dispersion loop the kinetic reaction loop cycles several times. The kinetics step in each cycle and for each box is described by

$$dC_1'/dt = (k_b C_n - k_t C_1^n) \xi_1 \quad (6)$$

$$-dC_n'/dt = dC_1'/dt \quad (7)$$

where  $C_1'$  is written in mg/ml and  $k_t$  and  $k_b$  are in the corresponding units. Notice that it is  $dC_n'/dt$  and not the corresponding thermodynamic concentrations. This is because the mass within a single box is

$$C_T' A dx = (C_1' + C_n') A dx = (C_1 \xi_1 + C_n \xi_n) A dx = C_T \bar{\xi}_w A dx \quad (8)$$

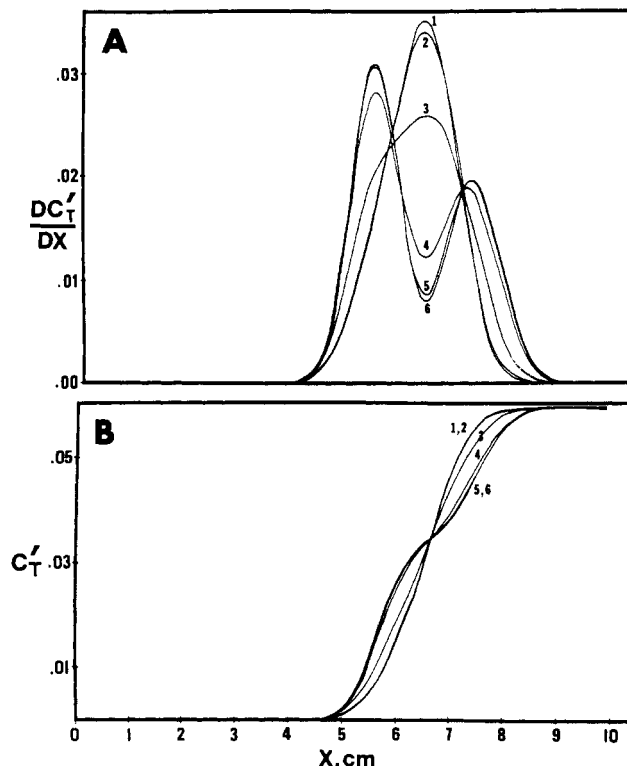


FIGURE 4: Effect of stoichiometry on kinetic parameters. Computer simulations of reaction profiles for a monomer-dimer system after 192 min at a flow rate of 1.2 ml/hr on Sephadex G-100R. The initial concentration of the mixture is 0.1 mg/ml and is 50% dimer (by weight). Interaction parameters are (1) instantaneous equilibrium,  $K_{eq} = 20 \text{ (mg/ml)}^{-1}$ ; (2)  $k_t = 2.0 \text{ (mg/ml)}^{-1} \text{ min}^{-1}$ ,  $k_b = 0.1 \text{ min}^{-1}$ ; (3)  $k_t = 0.2 \text{ (mg/ml)}^{-1} \text{ min}^{-1}$ ; (4)  $k_t = 0.02 \text{ (mg/ml)}^{-1} \text{ min}^{-1}$ ,  $k_b = 0.001 \text{ min}^{-1}$ ; (5)  $k_t = 0.002 \text{ (mg/ml)}^{-1} \text{ min}^{-1}$ ,  $k_b = 10^{-4} \text{ min}^{-1}$ ; (6) no interaction. Curves A are derivatives of concentration profiles B.

where the unprimed concentrations  $C_1$ ,  $C_n$ , and  $C_T$  are the bulk (thermodynamic) concentrations.  $A$  is the cross-sectional area of the column and  $dx$  is the linear distance increment. After reaction the conservation of mass dictates that  $C_T'$  remain constant while  $C_1'$ ,  $C_n'$ ,  $C_1$ , and  $C_n$  may change. Because  $C_1$  and  $C_n$  change,  $\bar{\xi}_w$  changes and, therefore,  $C_T$  must change. This implies that the proportion of each species within both the void volume and the internal volume changes during the reaction.

The computer program, as it now exists, is capable of handling any four components with any combination of instantaneous equilibrium interactions, kinetically controlled interactions, and/or lack of interactions. The number of components can, of course, be expanded by simply increasing the storage area required by the program.

The parameters used for these simulations are given in Table I. The manner in which these parameters were derived is given in Zimmerman and Ackers (1971a) and Zimmerman *et al.* (1971) based on values derived by Halvorson and Ackers (1971). All reactions pertain to a system where the monomer is 17,000 daltons and has a radius of 18.9 Å. The radius of the  $n$ -mer is based on the model

$$a_n = a_1 n^{1/3} \quad (9)$$

where  $a_1$  is the radius of the monomer,  $a_n$  is the radius of the  $n$ -mer, and  $n$  is the degree of polymerization.

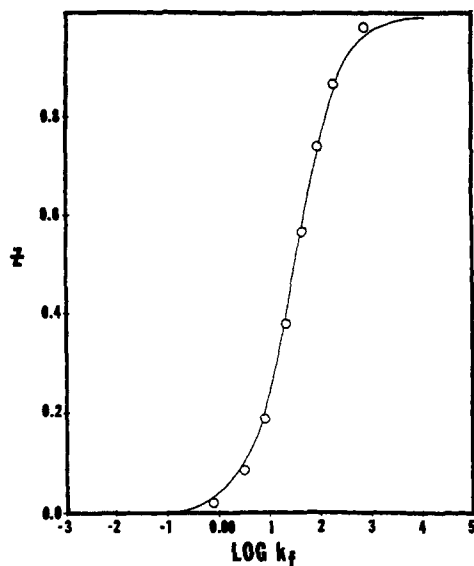


FIGURE 5: Derivative parameters as a function of kinetic constants. Open symbols are points generated by computer simulation. Solid curve is best fit of eq 12 with  $L$  having a value of  $28.8 \text{ (mg/ml)}^{-3} \text{ min}^{-1}$  ( $\log L = 1.46$ ). The values of the rate constant shown are for the forward reaction, but the same curve would be generated for the backward reaction if  $\log(8000)$  is subtracted from the values shown.

## Results and Discussion

Figure 1 represents a monomer-tetramer system on Sephadex G-200 initially at equilibrium, 50% (on a weight basis) being tetramer. The forward and reverse rate constants were varied, as shown, always maintaining a ratio equal to the equilibrium constant ( $8000 \text{ (mg/ml)}^{-3}$ ). For the example given, there is no significant deviation from instantaneous equilibrium until the forward rate constant drops below  $800 \text{ (mg/ml)}^{-3} \text{ min}^{-1}$ . When the forward rate becomes less than  $0.80 \text{ (mg/ml)}^{-3} \text{ min}^{-1}$  the resulting curve is essentially indistinguishable from no interaction between monomer and tetramer.

Figures 2 and 3 also show monomer-tetramer interactions but for 90 and 10% tetramer, respectively, in the initial equilibrium mixture. Here the differences are much less apparent because one of the components is initially present in relatively small quantities, making the difference between "rapid" and "slow" interactions much less obvious. There is, however, only a relatively small range of rate constants over which this transition takes place.

It is not immediately apparent as to the best criteria upon which to compare systems with differing stoichiometries and initial compositions. One common feature of the monomer- $n$ -mer interaction given by reaction III is that the dissociation reaction is first order and therefore the half-time is not dependent upon concentration. Another method would be to compare half-times of the association reaction by the equation

$$t_{1/2} = \frac{(2^n - 1)}{(n - 1)} \frac{1}{k_t} \frac{1}{C_0^{n-1}} \quad (10)$$

where  $n$  is the degree of association,  $k_t$  is the association rate constant, and  $C_0$  is the thermodynamic concentration of the  $n$ -mer in the initial mixture. One similarity between all three systems is immediately obvious. In the region where the dissociation rate constant is near a value of  $0.01 \text{ min}^{-1}$ , the boundary profile is in a region where control is kinetic. This

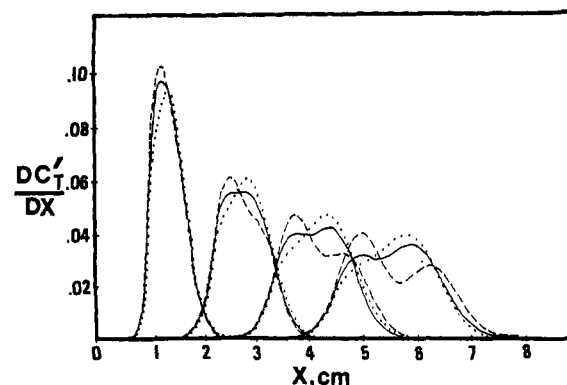


FIGURE 6: Time dependence of reaction profile: curve 1 (.....) is for instantaneous equilibrium; curve 2 (—) for the kinetically controlled case with  $k_t = 80 \text{ (mg/ml)}^{-3} \text{ min}^{-1}$ ; and curve 3 (---) for the case where no interaction occurs. All cases refer to the monomer-tetramer system initially containing 50% tetramer at an initial total concentration of  $0.1 \text{ mg/ml}$ . The four times are 48, 96, 144, and 192 min on a Sephadex G-2000R column at a flow rate of  $1.2 \text{ ml/hr}$ . Derivative profiles only are shown.

first-order rate constant describes a reaction with a half-time of 69 min.

If this generalization based on three monomer-tetramer systems is indeed valid, then one would expect other stoichiometries to also show kinetically controlled profiles when the dissociation rate constant is  $0.01 \text{ min}^{-1}$ . Figure 4 shows the reaction profile for a monomer-dimer system on Sephadex G-100 with varying rate constants. Again one can see that the most significant deviation from both instant equilibrium and no interaction is when the dissociation rate is  $0.01 \text{ min}^{-1}$ . By changing systems we have changed stoichiometries as well as gels. As a result, velocity and dispersion parameters also are changed, yet the basic observation remains true.

In Figures 1–4, the rate constants are varied by powers of ten to define an approximate range of effect. In an attempt to gain more insight into the area where kinetic control is important, the kinetic parameters of the system in Figure 1 (initially 50% tetramer, 50% monomer,  $k_t/k_b = 8000 \text{ (mg/ml)}^{-3}$ ) were varied so that a range of  $k_t$  values were simulated. The results are plotted in Figure 5 with the log of these intermediate values plotted against values of  $Z$ , where  $Z$  is a coordinate defined by the following equation

$$Z = \frac{(dC'/dX)_x - (dC'/dX)_{x_N}}{(dC'/dX)_{x_{eq}} - (dC'/dX)_{x_{N1}}} \quad (11)$$

where  $(dC'/dX)_x$  is the value of the derivative curve generated by any set of rate constants at some constant reference point  $X$ ,  $(dC'/dX)_{x_{N1}}$  is the value of the derivative curve for the noninteraction case at reference point  $X$ , and  $(dC'/dX)_{x_{eq}}$  is the value of the derivative curve for the instant equilibrium case at reference point  $X$ . The reference point  $X$  was arbitrarily chosen to be the minimum of the derivative curve in the noninteracting case since the difference between the instant equilibrium and noninteraction cases appears to be the largest at this point. From these curves, one can see that the shape of the reaction profile for this case is kinetically controlled between values for the association rate constant of 640 and  $0.8 \text{ (mg/ml)}^{-3} \text{ min}^{-1}$ , corresponding to dissociation rate constants of 0.08 and  $0.0001 \text{ min}^{-1}$ , respectively. An

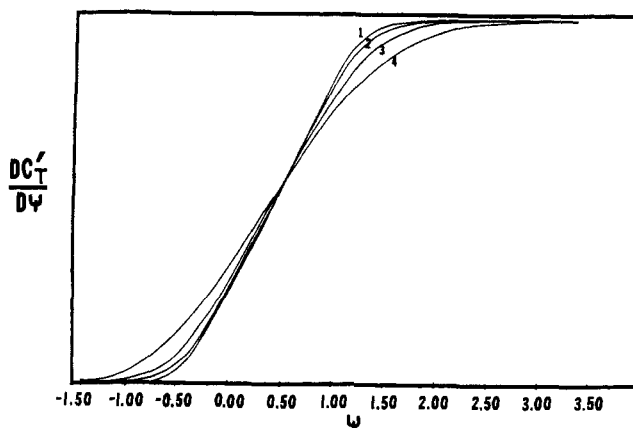


FIGURE 7: Time independent reaction profile. The kinetically controlled case (curve 2) from Figure 6 is reduced to the time-independent coordinate system defined by 13. Times are (1) 48 min, (2) 96 min, (3) 144 min, and (4) 192 min.

observation, in this case, is that the curve may be fit extremely well by the equation

$$L = k_t \frac{1 - Z}{Z} \quad (12)$$

where  $Z$  is the same as previously defined, and  $L$  is some constant. In this case the value of  $L$  that gives the best fit is  $28.8 \text{ (mg/ml)}^{-3} \text{ min}^{-1}$  ( $k_b = 3.6 \times 10^{-3} \text{ min}^{-1}$ ), which corresponds to a half-time of dissociation of 192 min. The source of this agreement may be merely coincidence; however, since the perturbation of the equilibrium in this type of experiment is created by dilution, it does seem that the governing rate of reaction should be the relaxation toward equilibrium.<sup>2</sup>

In Figure 6 are compared the derivatives of the time dependency of the reaction profiles for three different rates of reaction, instantaneous equilibrium, an association reaction rate of  $80 \text{ (mg/ml)}^{-3} \text{ min}^{-1}$ , and for no interaction. All pertain to the same initial conditions of 50% tetramer, 50% monomer (by weight), and an initial total concentration of 0.1 (mg/ml). The difference in the profiles in the area where the slower species would predominate becomes apparent almost immediately. Differences in this region also mirror the results demonstrated by Figure 5; however, the absolute magnitude of the differences between no interaction and instantaneous equilibrium are different at each stage. If the profile were measured at a much later time or a much earlier time the differences would not be so apparent. Since the longest time shown (192 min) is only four times the smallest time shown (48 min), the time on the column in each case is within an order of magnitude of the half-time (69 min) of the back reaction described by  $k_b$  and therefore observable.

Figure 7 shows another unexplained phenomena that has been noted by us before (Zimmerman and Ackers, 1971a, 1973); and by others for countercurrent distribution (Bethune, 1970; McNeil *et al.*, 1970). When a single system is analyzed at several times and the resulting profiles are normalized to a time-independent coordinate, one sees a hinge point. The time-independent coordinate system we use is

$$\psi = \frac{X - Ft/\xi_1}{Ft/\xi_n - Ft/\xi_1} \quad (13)$$

<sup>2</sup> The author wishes to thank Dr. D. J. Cox for pointing this out.

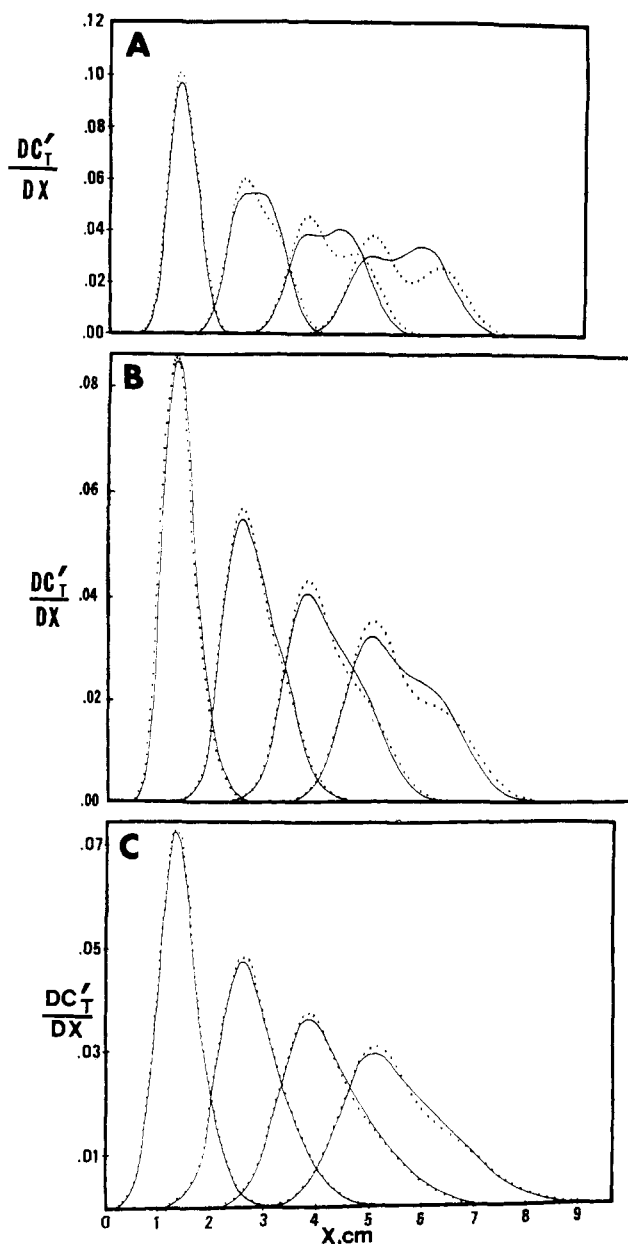


FIGURE 8: Time dependency as a function of flow rate. All systems refer to a monomer-tetramer initially containing 50% tetramer at an initial concentration of 0.1 mg/ml. Curve A has a flow rate of 1.2 ml/hr with times of 48, 96, 144, and 192 min. Curve B is for a flow rate of 4.8 ml/hr for times of 12, 24, 36, and 48 min. Curve C is for a flow of 9.6 ml/hr for times of 6, 12, 18, and 24 min. In all cases, the solid curves refer to the kinetically controlled case with  $k_t = 80 \text{ (mg/ml)}^{-3} \text{ min}^{-1}$ . The dotted curves refer to the corresponding non-interaction cases. In all cases only the derivative patterns are shown.

where  $X$  is the distance parameter,  $Ft/\xi_1$  represents the distance moved by monomer, and  $Ft/\xi_n$  represents distance moved by the  $n$ -mer after time  $t$ . The only systems in which this hinge point seems to be missing are with certain noninteracting species (J. K. Zimmerman, unpublished results). It is present in every rapid equilibrium system examined so far.

It would be quite nice if one could go back from experimentally observed curves to calculate kinetic constants. It might appear that by varying the flow rate of the system and thus varying the time allowed for reaction one could do this crudely. However, despite the many advantages gel chromatography possesses because of the importance of dispersion

TABLE II: Effect of Flow Rate on Dispersion Parameters.

Flow Rate (ml/hr)	$L_1$ (cm <sup>2</sup> /min)	$L_n$ (cm <sup>2</sup> /min)
1.2	$3.61 \times 10^{-4}$	$4.86 \times 10^{-4}$
4.8	$2.11 \times 10^{-3}$	$4.51 \times 10^{-3}$
9.6	$6.38 \times 10^{-3}$	$1.60 \times 10^{-2}$

on the shape of the profile, this very blessing becomes a curse in that the variation of flow rate also completely changes the pattern of the reference cases as shown in Figure 8. Table II shows the parameter  $L$  for each species is changed resulting in the gross effect on the resulting curves shown in Figure 8. Therefore, for comparison, one must know all of the appropriate parameters at each flow rate, exactly the information one is looking for. Right now, the best method seems to be to initialize the simulation with experimental data and compare data gathered at a later time with that simulated. The appropriate parameters can then be adjusted and the simulation attempted again. Further work on analysis by the variation of flow rates does seem to have certain promise as seen in Figure 8 and is being pursued.

Reaction profiles shown here indicate that kinetic control of reversible association-dissociation reaction occurs when the system under study has a dissociation rate constant giving a half-time within 1–1.5 orders of magnitude of the time the macromolecular system has been undergoing transport. However, these observations are based on only four systems, and more work must be done to establish the universal validity of this conclusion. Using this observation it appears that even with the difficulty described above, one should be able to vary the flow rates used in the chromatography of such systems and eventually extract information concerning the rate constants of a given experimental system. This type of analysis will still have to await the development of the appropriate theoretical treatment.

#### Acknowledgments

The author wishes to thank Dr. G. K. Ackers of the University of Virginia for his constant help and encouragement during the duration of this work. The author also wishes to thank the Computer Science Center of Clemson University for the gift of enormous amounts of computer time.

#### References

- Ackers, G. K. (1970), *Advan. Protein Chem.* 24, 343.  
 Belford, G. G., and Belford, R. L. (1962), *J. Chem. Phys.* 37, 1926.  
 Bethune, J. L. (1970), *J. Phys. Chem.* 74, 3837.  
 Bethune, J. L., and Kegeles, G. (1961), *J. Phys. Chem.* 65, 433.  
 Brumbaugh, E. E., and Ackers, G. K. (1968), *J. Biol. Chem.* 243, 6315.  
 Cann, J. R. (1970), *Interacting Molecules. The Theory and Practice of Their Electrophoresis, Ultracentrifugation, and Chromatography*, New York, N. Y., Academic Press.  
 Cann, J. R., and Goad, W. B. (1965), *J. Biol. Chem.* 240, 148.  
 Cann, J. R., and Goad, W. B. (1972), *Arch. Biochem. Biophys.* 153, 603.  
 Cann, J. R., and Oates, D. C. (1973), *Biochemistry* 12, 1112.  
 Cox, D. J. (1965), *Arch. Biochem. Biophys.* 112, 249, 259.  
 Cox, D. J. (1967), *Arch. Biochem. Biophys.* 119, 230.  
 Cox, D. J. (1969), *Arch. Biochem. Biophys.* 129, 106.  
 Cox, D. J. (1971), *Arch. Biochem. Biophys.* 142, 514.  
 Gilbert, G. A. (1955), *Discuss. Faraday Soc. No. 20*, 68.  
 Gilbert, G. A. (1959), *Proc. Roy. Soc., Ser. A* 250, 377.  
 Gilbert, G. A., and Jenkins, R. C. L. (1956), *Nature (London)* 177, 853.  
 Gilbert, G. A., and Jenkins, R. C. L. (1959), *Proc. Roy. Soc., Ser. A* 253, 420.  
 Halvorson, H. R., and Ackers, G. K. (1971), *J. Polym. Sci., Part A* 29, 245.  
 Halvorson, H. R., and Ackers, G. K. (1973), *J. Biol. Chem.* (in press).  
 Longworth, L. G., and MacInnes, D. A. (1942), *J. Gen. Physiol.* 25, 507.  
 McNeil, B. J., Nichol, L. W., and Bethune, J. L. (1970), *J. Phys. Chem.* 74, 3846.  
 Oberhauser, D. F., Bethune, J. L., and Kegeles, G. (1965), *Biochemistry* 4, 1878.  
 Van Holde, K. E. (1962), *J. Chem. Phys.* 37, 1922.  
 Zimmerman, J. K., and Ackers, G. K. (1971a), *J. Biol. Chem.* 246, 1078.  
 Zimmerman, J. K., and Ackers, G. K. (1971b), *J. Biol. Chem.* 246, 7298.  
 Zimmerman, J. K., and Ackers, G. K. (1973), *Anal. Biochem.* (in press).  
 Zimmerman, J. K., Cox, D. J., and Ackers, G. K. (1971), *J. Biol. Chem.* 246, 4242.